POLITECNICO DI TORINO
Repository ISTITUZIONALE

The effect of magnesium on bioactivity, rheology and biology behaviors of injectable bioactive glass-gelatin-3-glycidyloxypropyl trimethoxysilane nanocomposite-paste for small

(Article begins on next page)

17 July 2022

Ceramics International

The effect of Magnesium on bioactivity, rheology and biology behaviors of injectable bioactive glass-gelatin-3-glycidyloxypropyl trimethoxysilane nanocomposite-paste for small bone defects repair
--Manuscript Draft--

Manuscript Number:	
Article Type:	Full length article
Keywords:	Bioactive glass; Nanocomposite paste; Magnesium; Bone.
Corresponding Author:	Andrea Cochis, Ph.D. Università degli Studi del Piemonte Orientale Novara, ITALY
First Author:	Mehri Sohrabi
Order of Authors:	Mehri Sohrabi
	Bijan Eftekhari Yekta
	Hamidreza Rezaie
	Mohammad Reza Naimi-Jamal
	Ajay Kumar
	Andrea Cochis, Ph.D.
	Marta Miola
	Lia Rimondini
Abstract:	Injectable bioactive glass-based pastes represent promising biomaterials to fill small bone defects thus improving and speed up the self-healing process. Accordingly, injectable nanocomposite pastes based on bioactive glass-gelatin-3-glycidyloxypropyl trimethoxysilane (GPTMS) were here synthesized via two different bulk glasses containing 64SiO2, 27CaO, 4MgO, 5P2O5 (mol.%) or 64SiO2, 31CaO, 5P2O5 (mol.%). In particular, the effects of MgO on bioactivity, rheology, injectability, disintegration resistance, and cellular behaviors were investigated. The results showed that the disintegration resistance of the composite was improved by the replacement of MgO, thus leading to an increase in the amount of storage modulus (G') from 26800 to 43400 Pa, equal to an increase in the viscosity of the paste from 136 × 103 to 219 × 103 Pa.s. Since the release rate of ions became more controllable, the formation of calcite was decreased after immersion of the Mg bearing samples in the SBF solution. Finally, specimens' cytocompatibility was confirmed towards human osteoblasts by metabolic assay as well as the ability of human fibroblasts to penetrate within the pores of 3D composites was verified by a migration assay simulating the devices repopulation upon injection in the injured site.
Suggested Reviewers:	Francesco Baino Politecnico di Torino Dipartimento Scienza Applicata e Tecnologia francesco.baino@polito.it Expert in bioactive glass and ceramics develpopment and chemical characterization
	Oana Bretcanu Newcastle University oana.bretcanu@ncl.ac.uk Expert in bioactive glass chemistry
	Seiji Yamaguchi sy-esi@isc.chubu.ac.jp Expert in bioactive glasses modification for biomedical applications
Opposed Reviewers:	

<u>To the Editor of the *Ceramics International* Journal</u>

Dear Prof. P. Vincenzini,

we submitted for a possible consideration on the *Ceramics International* Journal the original article entitled "*The effect of Magnesium on bioactivity, rheology and biology behaviors of injectable bioactive glass-gelatin-3-glycidyloxypropyl trimethoxysilane nanocomposite-paste for small bone defects repair*" by Mehri Sohrabi, Bijan Eftekhari Yekta, Hamidreza Rezaie, Mohammad Reza Naimi-Jamal, Ajay Kumar, Andrea Cochis, Marta Miola and Lia Rimondini.

In this manuscript we demonstrated how the magnesium substitution in the bioactive glass composition can significantly improve the bioactivity, rheology and biology properties of injectable pastes aimed at small bone defects repair. Moreover, the presence of such "cells-friendly" polymer ameliorated the biological properties of the bioactive glass when used in direct contact with osteoblasts (MG63) and fibroblasts (HGF) cells, all involved in the self-healing process. Accordingly, we believe that the manuscript can be of interest for the readers of Your Journal.

Finally, we confirm that the manuscript is original, that it has been approved by all the Authors and that it is not actually under the evaluation of any other Journal.

Sincerely,
the corresponding Authors,

Prof. Bijan Eftekhari Yekta

Prof. Lia Rimondini

The effect of Magnesium on bioactivity, rheology and biology behaviors of injectable bioactive glass-gelatin-3-glycidyloxypropyl trimethoxysilane nanocomposite-paste for small bone defects repair

Mehri Sohrabi[1], Bijan Eftekhari Yekta[1,*], Hamidreza Rezaie[1], Mohammad Reza Naimi-Jamal[2], Ajay Kumar[3], Andrea Cochis[3], Marta Miola[4] and Lia Rimondini[3,*]

[1] School of Metallurgy & Materials Engineering, Iran University of Science and Technology, Tehran, Iran.

[2] Department of Chemistry Research laboratory of green organic synthesis and polymers, Iran University of Science and Technology, Tehran, Iran.

[3] Department of Health Sciences, Center for Translational Research on Autoimmune and Allergic Diseases–CAAD, Università del Piemonte Orientale UPO, Novara, Italy.

[4] Department of Applied Science and Technology, Politecnico di Torino, Turin, Italy.

* Correspondence:

Prof. Bijan Eftekhari Yekta

Iran University of Science and Technology, Tehran, Iran

e-mail: beftekhari@iust.ac.ir

Tel: +9821 73228873

Fax: +9821 77240480

Prof. Lia Rimondini

Università del Piemonte Orientale UPO, Novara, Italy

e-mail: lia.rimondini@med.uniupo.it

Tel: + 39 0321 660673

Fax: +39 0321 620421

Abstract

Injectable bioactive glass-based pastes represent promising biomaterials to fill small bone defects thus improving and speed up the self-healing process. Accordingly, injectable nanocomposite pastes based on bioactive glass-gelatin-3-glycidyloxypropyl trimethoxysilane (GPTMS) were here synthesized via two different bulk glasses containing $64SiO_2$, $27CaO$, $4MgO$, $5P_2O_5$ (mol.%) or $64SiO_2$, $31CaO$, $5P_2O_5$ (mol.%). In particular, the effects of MgO on bioactivity, rheology, injectability, disintegration resistance, and cellular behaviors were investigated. The results showed that the disintegration resistance of the composite was improved by the replacement of MgO, thus leading to an increase in the amount of storage modulus (G') from 26800 to 43400 Pa, equal to an increase in the viscosity of the paste from 136×10^3 to 219×10^3 Pa.s. Since the release rate of ions became more controllable, the formation of calcite was decreased after immersion of the Mg bearing samples in the SBF solution. Finally, specimens' cytocompatibility was confirmed towards human osteoblasts by metabolic assay as well as the ability of human fibroblasts to penetrate within the pores of 3D composites was verified by a migration assay simulating the devices repopulation upon injection in the injured site.

Keywords: Bioactive glass; Nanocomposite paste; Magnesium; Bone.

1. Introduction

Between the class of bone substitute, bioactive glasses (BG) represent a very promising category; thanks to their biocompatibility and bioactivity towards the host tissue, they may be used as porous scaffolds, fillers, dental grafts, coatings, and orthopedic implants [1-3]. BG bioactivity is due to their chemical similarity to the bone tissue; so, BG easily attach to the bone by forming a layer of hydroxycarbonate apatite (HCA) on its surface [1]. This process, which begins with the release of cations and the formation of silica hydrate finishes after the formation of a crystalline hydroxyapatite layer [4], according the following steps:

i) Replacement of Mg^{2+}, Na^+, and Ca^{2+} cations with H^+ in the medium and hydrolysis of the silica groups and the formation of silanols ($Si-O-Na^+ + H^+ + OH^- \rightarrow Si-OH^+ + Na^+ + OH^-$)

ii) Once the hydroxyl groups amount in the medium increases, the silica network attach and the silica bond is broken ($Si-O-Si + H_2O \rightarrow Si-OH + Si-OH$)

iii) Condensation of Si-OH groups, polymerization of silica-rich layers, and release of alkaline and alkaline earth ions

iv) Migration of Ca^{2+} and PO_4^{3-} ions on the surface of the silica-rich layer and the formation of a $CaO-P_2O_5$ amorphous layer on its surface.

v) Crystallization of a $CaO-P_2O_5$ layer and the formation of crystalline hydroxyapatite carbonate

The precipitated HCA can bond with collagen fibers thus providing an adequate surface for adhesion and proliferation of osteogenic cells, creating a bridge with the bone [1].

Taking onto account the class of injectable pastes for bone small defects repair, it must be considered that BG are often used in combination with other biopolymers to improve mechanical properties. Accordingly, by a combination of degradable polymers such as chitosan, gelatin, sodium alginate or hyaluronic acid with a bioactive glass powder, an appropriate bioactive composite can be formed known as organic-inorganic hybrids [5,6]. The choice of the most appropriate polymer depends by the biocompatibility, the lack of side effects upon implantation (such as inflammation or allergy) and the physical-chemical properties such as degradation and reabsorption [7-11]. In particular, gelatin seems to hold such characteristics as it has been used for many applications including the synthesis of hydrogels, composites hybrids and scaffolds [12,13]. Thanks to the gelatin high affinity with cells, the presence of such polymer can be exploited to improve cells adhesion, spread, differentiation and proteins expression onto materials with low bioactivity or aimed at tissue healing. Accordingly, the use of gelatin as co-polymer can be applied towards injectable bioactive glass-based pastes for small bone defect repair developing composites with high bioactivity and injectability.

However, a predictable limitation of bioactive glass-gelatin composites is due to their sensitivity towards temperature that can cause poor stability upon injection in the body [14,15]. Therefore, to solve this problem, an appropriate cross-linker should be used as third component to improve the stability of the composites. Various materials such as polyethilenglicol, β-glycerophosphate, glutaraldehyde, hydroxyl propyl and methylcellulose, have been used as cross-linker for glass-polymer composites [16-20]. Trimethoxysilane

3

(3-glycidyloxypropyl) (GPTMS) is a biocompatible cross-linker forming silanol groups by hydrolyzing its methoxy groups leading to a silicate network [21]; due to the presence of such silanol groups, GPTMS can give rise to a strong bond with gelatin [22]. Moreover, the organic-inorganic compound derived from GPTMS cross-link can display ameliorate physical and chemical properties and a higher stability of the mineral and organic components [22].

Another key factor influencing the glass kinetics and the formation of the hydroxyapatite layer is the glass' chemical composition [23-25]. So far, the effect of oxides such as Ag, P, F, ZrO_2, Al, Zn, Sr, and Mg on the biological, physical, and chemical properties of such glasses have been studied [26-33]. In particular, magnesium seems holding the capacity to strongly influence the glass kinetics. The addition of MgO up to 13 mol.% into glass can delay the apatite formation without inhibiting the process as well as an increase of the alkaline phosphate activity (ALP) can be observed thus improving osteoblasts proliferation [34,35]. Besides, Mg ions affects the bone matrix quality as demonstrated by the evidence that its deficiency can causes bone fractures [34,35]. Despite these positive evidences, the role of magnesium influencing the physical-chemical behavior of the glass is still debated in literature. In fact, magnesium has been found to be a modifier element in several studies [36], although others have suggested that magnesium is an intermediate oxide entering the silica network as MgO_4 [27,37]. Therefore, there are contradictory results about the effect of magnesium oxide on the glass properties. Some researchers have shown that MgO delays the apatite layer's mineralization through reducing the mineral layer's thickness [38-40]. Some other studies have shown that the presence of MgO has no effect on the formation of the hydroxyapatite layer, but rather stimulates and promotes the early stages of mineralization [41,42]. Also, it has been found that the substitution of MgO with CaO can improve the stability as well as the mechanical properties of the glass [43].

Dealing with the ions influence on the glass behavior, in a prior work the Authors found that in a glass-gelatin injectable paste composite, an extra amount of Ca^{2+} ions determined the precipitation of calcite instead of apatite, when the injectable paste was tested by immersion in Simulated Body Fluid (SBF) solution [15]. Here, the role of magnesium was investigated in terms of mechanical, chemical and biological properties influence by comparing bulk $64SiO_2$-$31CaO$-$5P_2O_5$ (mol.%) bioactive glasses and Mg-doped $64SiO_2$-$27CaO$-$4MgO$-$5P_2O_5$ (mol.%) glasses aimed at injectable pastes for small bone defects repair. The pastes were investigated for their mechanical properties, injectability and bioactivity, while cytocompatibility was tested towards osteoblasts and fibroblasts in a migration assay. Results suggested that by adding Mg to the bioactive glass the release of Ca^{2+} was controlled thus avoiding the formation of calcite, bringing to a general improvement of the tested mechanical, chemical and bioactive properties.

2. Materials and Methods

2.1 Composites preparation

4

Two bioactive glasses $64SiO_2$-$31CaO$-$5P_2O_5$ mol.% (BG) and $64SiO_2$-$27CaO$-$4MgO$-$5P_2O_5$ mol.% (BG-Mg) were synthesized through the acid-base sol-gel method as previously described [10]. The precursors triethyl phosphate (TEP), tetraethyl orthosilicate (TEOS), calcium nitrate tetrahydrate powder, magnesium nitrate, ammonia solution, and nitric acid solution were purchased from Merck (Merck KGaA, Darmstadt, Germany) while bovine gelatin (Gel) and (3-Glycidyloxypropyl) trimethoxysilane (GPTMS) were purchased from Sigma (Sigma-Aldrich, St. Louis, USA). To prepare the gelatin solution, 3 wt.% gelatin powder was dissolved in distilled water. To prepare the composite pastes, the bioactive glass powder was mixed with the polymer solution and the GPTMS according to the amount detailed in Table 1, with a powder to liquid ratio (P/L) of 0.25 (referring powder to the glass and liquid to the polymer solution). As a result, two different pastes BG-Mg-Gel and BG-Gel were prepared, with the same powder-to-liquid ratio; finally, 20 wt.% (to the dry weight of polymer powder) GPTMS was added to each of them.

2.2 Physical-chemical characterization

2.2.1 Morphology and composition analysis

Composites' surface area, pore size and pore volume were determined by the Brunauer-Emmett-Teller (BET) analysis using an ASAP 2020 instrument (from Micromeritics Instrument Corporation, GA, USA) at 77K with nitrogen as absorbent. Glass powder phase specifications were measured using an X-ray diffractometry (XRD), with Cu-Kα radiation and X-ray wavelength of 1.54050 Å (Dron 8, Bourevestink, Russia), operated at 40 kV and 40 mA at a step size of 0.04 and a count time of 2 s/step. The morphology of the glass particles was studied by scanning electron microscopy (SEM, TEScan, VeGa II, Czech).

2.2.2 Mechanical properties evaluation

Rheology was applied to evaluate pastes' mechanical properties using a MC-R300 rheometer with a plate-plate geometry device (from Anton Paar GmbH, Graz, Austria). The test was carried out at room temperature in an oscillatory mode, whereby 3 g of the paste was placed on the bottom plate of the device 1 mm distant from the top plate. To determine the linear viscoelastic region, the storage (G') and the loss (G") modules were measured in terms of strain (γ), while the complex viscosity (η*), G' and G" were determined in terms of angular frequency (ω).

2.2.3 Pastes injectability and disintegration resistance

To measure the injectability of the pastes, 3 g of each paste was poured into the syringe with a needle diameter of 2 mm, and a compressive force was applied on the syringe's piston under the speed of 30 mm/min, using a computer-controlled mechanical testing machine (SANTAM STM-20). Finally, the compressive force versus displacement was measured, and the percentage of injectability was calculated according to the following equation 1 (Eq.1):

$$(Eq.1) \ Injectability(\%) = \frac{Extruded \ paste \ volume}{Total \ paste \ volume} \times 100$$

The pastes were immersed in the simulated body fluid (SBF) solution, which was developed based on Kokubo's method [44] and placed at 37 °C in the incubator for 5 min, 24 h, and 48 h, respectively, to determine their disintegration resistance (Dr). Dr was calculated according to the equation 2 (Eq.2) where Ws is the disintegrated paste weight after removing the SBF solution while Wi is the total paste weight before immersion.

$$(Eq.2) \ Dr = \frac{Wi - Ws}{Wi} \times 100$$

2.2.4 Pastes bioactivity evaluation

Pastes' bioactivity was evaluated by their ability to form apatite *in vitro*. Accordingly, 1 g of each paste was immersed in 30 ml of the SBF solution at 37 °C in an incubator. The solution was refreshed every 48 h up to 14 days. At each time points, the pastes were taken out from the solution, rinsed with distilled water and air-dried at room temperature. To demonstrate the phase composition of the pastes, before and after immersion in the SBF solution, the dried pastes were analyzed by XRD whereas the morphology and chemical composition of the particles in the pastes, before and after immersion, was visually checked by SEM-EDX. The chemical band groups in the pastes were studied by Fourier Transform Infrared Spectroscopy (FTIR) at a wavelength of 4000-400 cm^{-1} with KBr pellets.

2.3 Biological evaluation

2.3.1 Cytocompatibility

Specimens were UV-sterilized (30 minutes/each side) and molded into 1 cm diameter, 1 cm height disks prior to perform biological assays. Human mature osteoblasts (MG-63, ATCC CRL-1427) were purchased from the American Type Culture Collection (ATCC, Manassas, USA) and used as bone-like model to test pastes cytocompatibility *in vitro*. Cells were cultivated into Dulbecco's Modified Minimal Essential Medium (DMEM, from Sigma-Aldrich) supplemented with 10% fetal bovine serum (FBS) and 1% antibiotics (penicillin/streptomycin) at 37 °C in a 5% CO_2 atmosphere. After reaching 80-90% confluence, cells were detached by trypsin-EDTA solution, harvested and directly drop-wise seeded onto specimens' surface at defined concentration ($1x10^4$ cells/specimen). Composites were incubated (37°C, 5% CO2) for 24 and 72 hrs; at each time-points, cells' viability was determined by the metabolic colorimetric alamar blue assay (Alamar Blue™, from Life Technologies, ThermoFisher, USA) following Manufacturer's instructions. Briefly, supernatants were removed from each well containing cells and replaced with the alamar blue solution (10% v/v in fresh medium). Plates were incubated in the dark for 4 hours and then 100 µl were removed, spotted into a new black 96-well plate and fluorescence signals were evaluated with a spectrophotometer (Spark,

Tecan Trading AG, CH) using the following set-up: fluorescence excitation wavelength 570 nm, fluorescence emission reading 590 nm. Finally, cells morphology was visually evaluated by SEM observations after 72 hrs cultivation. Briefly, samples were washed twice with phosphate-buffered saline (PBS), fixed for 12 hrs by 4% formaldehyde and dehydrated by the alcohol scale (50%, 70%, 90%, and 100%, 2 hrs each). Subsequently, dehydrated specimens were surface covered with conductive silver and examined by SEM imaging.

2.3.2 Migration assay

To evaluate the pastes' ability to support new tissue ingrowth within pores simulating the self-healing process, a migration assay was performed using human primary fibroblasts (HGF, ATCC PCS-201-018). Accordingly, 8 mm height - 4 mm width cylinders were realized and sterilized by UV light. Cells were purchased from ATCC and cultivated into alpha-modified DMEM (α-MEM, from Sigma) supplemented with 10% FBS and 1% antibiotics. Once cells reached 80-90% confluence, they were detached by trypsin-EDTA a seeded onto specimens' top side embedded into 20 μl of a collagen matrix (PureCol™ EZ Gel solution, from Sigma) used as a temporary substrate. After collagen gelation (2 hrs, 37 °C) the specimens were rinsed with fresh medium (1 ml each) and cultivated for 15 days with medium changed every 3 days. Finally, specimens were collected, vertically cut into 2 halves to visualize the internal part, dehydrated by the alcohol scale, covered with Cr and observed with a JEOL NEOSCOPE JCM 6000 PLUS SEM (from Nikon Instrument S.p.A., Firenze, Italy).Images of the internal part were used to confirm cells' migration from the top side within the pores.

2.4 Statistical analysis of data

Biological experiments were performed using 6 replicates. Samples were statistically compared by the SPSS software (v25, IBM) using the one-way ANOVA test after check of normal distribution and homogeneity using Shapiro-Wilk's and Levene's test respectively. Tukey's test was used for post-hoc analysis. Differences were considered as significant for $p < 0.05$.

3. Results and Discussion

3.1 Physical-chemical characterization

3.1.1 Composites morphology and structural characterization

The morphology, absorption-desorption curves, and X-ray diffraction patterns of the samples' BG and BG-Mg were investigated firstly (results are summarized in Table 2). The average particle size of BG and BG-Mg glasses resulted of approximately 50 nm and 100 nm, respectively. The hysteresis BET loops, according to the IUPAC classification, indicated that the two glasses were mesoporous. Based on the BJH adsorption – desorption traces, the pore volume, the specific surface area, and the size of average pores of BG and BG-

Mg resulted of 0.602 and 0.634 (cm^3/g), 123.139 and 109.104 (m^2/g), and 18.217 and 23.036 (nm), respectively. The XRD results represented that the samples were amorphous.

3.1.2 Composites injectability and disintegration resistance

Pastes injectability was studied under computer-controlled conditions by applying a compressive force towards 2 mm needle syringe lodging the composites. Accordingly, the injected volumes % and the relative applied forces required to complete the pastes extrusion are summarized in Table 3. Apparently, the entering of 4 mol.% Mg ions into the glass composition has not influenced the injectability at all. So, it can be speculated that the flow ability of the pastes is more dependent on the gelatin solution rather than to the glass composition [15].

After evaluating the role of Mg in the pastes injectability properties, the disintegration resistance (Dr) was selected as the second parameter to evaluate Mg contribute. Accordingly, pastes were immersed in SBF for 5, 24 and 48 hours prior to evaluate their Dr in comparison to the starting values as prior described in the Equation 1. Results are reported in Figure 1a showing that the resistance of the BG-Gel-GPT20 decreased more rapidly than the Mg-doped ones starting from 24 hrs immersion (97±2% vs 95±2%) and being more evident after 48 hrs (94±3% vs 89±3%). However, both pastes showed acceptable resistance and preserved their shapes after 48 h immersion. The difference between the two samples was attributed to the presence of magnesium in the BG-Mg-Gel-GPT20 structure. In fact, the pastes' Dr depends on two main factors: i) the cross link between the polymer chains due to the ions released from the glass (schematized in Fig. 1b) and ii) the bridging between the polymer and the glass (schematized in Fig. 1c). So, the glass particles can link the polymer molecules through i) $O^{-1}_{gelatin}$-M^{2+}-$O^{-1}_{gelatin}$ and/or ii) $O^{-1}_{gelatin}$-M^{2+}_{glass}-$O^{-1}_{gelatin}$ bonds and increase the disintegration resistance of the paste (M^{2+} refers to a two-valence cation like Ca^{2+} and/or Mg^{2+}). Magnesium plays a significant role in stabilizing the glass structure [34] and ameliorating the bond strength of the mentioned links. A glass forms a more strong and stable three-dimensional network when the ionic field strength of its cation increases, i.e. z.e/r2, where z,e, and r are the electrical valence of the cation, the electrical charge of the electron, and the ionic radius of the used modifier cation, respectively. The arrangement of ionic field strength for alkaline earth elements is Mg > Ca > Sr > Ba. It was also noted that the addition of MgO instead of CaO into the glass led to increase the network coherence attributed to the small size and larger field strength [45]. Thus, it can be concluded that the paste will be more resistant against disintegration when its glass constituent contains magnesium oxide. The reduction in the amount of calcite that is formed in the Mg-free sample seems to be another parameter that increases the disintegration resistance of BG-Mg-Gel-GPT20. Apparently, with the formation of calcium carbonate, the concentration of calcium ions in the solution is reduced, leading to a decrease in its probability for participation of the cross-linker in the paste.

8

3.1.3 Rheological characterization

Another key element of the injectable pastes is represented by their mechanical strength. As a temporary substrate for bone repair, it is very important that the pastes can support the imposed compressive and shear forces meanwhile the self-healing occurs forming the new bone. Accordingly, here the GPTMS was used as cross-linker to improve the stability and thus the mechanical strength of the gelatin-bioactive glass composites. In fact, as schematized in Figure 2a, gelatin can bind the GPTMS silanol groups to form a large proteins chain. Moreover, it can be considered that hydrogen, ionic and covalent bonds can be formed between the bioactive glass and gelatin, through i) the bond between silanol in the glass-amine and gelatin hydroxyl groups, ii) calcium/magnesium in the glass–carboxyl groups of gelatin, and iii) calcium/magnesium in the glass-oxygen in the gelatin. Taken into account such interactions, the rheological behavior of the injectable pastes was studied to investigate the effect of magnesium addition on this regard.

In Figure 2b the changes in the storage and loss modulus of the samples in different angular frequencies, determined at a constant strain of 0.3% were shown. The storage modules of both samples are higher than the loss modules in the whole frequency ranges. Conversely, a non-homogeneous pattern was found in the sample lacking a cross linker in a previous study from the Authors [15]. This behavior can be attributed once again to the presence of the cross-linker which contributes creating a coherent and integrated structure, as was previously observed in the disintegration resistance evaluation. The presence of Mg is expected to increase the strength of the glass by creating stronger Mg-O-Si bonds than that of the Ca-O-Si; therefore, the storage modules of the Mg bearing paste should be higher than the Mg-free one due to the material's elastic nature. The results of the rheology test, which are given in Table 4, seem to confirm these hypotheses.

Finally, in Figure 2c the reduction in the complex viscosity of the two samples by increasing the angular frequency, at a constant strain of 0.3%, suggested for a shear-thinning behavior of the pastes. The complex viscosity of the pastes depends on the paste's modules. Therefore, it can be speculated that the MgO-containing paste has a higher viscosity than the MgO-free one, which originates from their higher bond strength as noted before.

3.1.4 Bioactivity evaluation

The Mg-induced bioactivity was evaluated as the ability of the injectable pastes to form apatite instead of calcite as previously observed for calcium [15]. Accordingly, the XRD patterns before (0 day) and after immersion in the SBF of the two pastes are given in Figure 3a after 1 and 14 days. As can be observed, negligible peaks of calcite can be observed before and after the immersion of the Mg containing sample in the SBF (BG-Mg-Gel-GPT20), while calcite (reference code 00-001-837) is the main crystalline phase precipitated in the Mg-free sample, due to the higher amounts of calcium oxide in its glass phase. The reaction between Ca^{2+} ions and the CO_3^{2-} deriving from the polymers occurring in the SBF environment causes calcite precipitation as described in the Equation 3 (Eq.3):

$$(Eq.3)\ Ca^{2+} + 2HCO_3^- \rightarrow CaCO_3 + CO_2 + H_2O$$
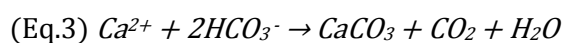
Similar to the results here obtained, Seah et al. [46] shown that in the 45S5 glasses calcite is formed in a highly concentrated homogeneous phase in the early days after immersion in SBF; however, it decomposes gradually with time releasing calcium ions into the SBF solution and thus participating in the formation of calcium phosphate. The highest intensity peak of apatite was observed for both pastes after 14 days of immersion; however, apatite was found to precipitate later in the Mg-containing paste in comparison to the bulk materials. In a previous study, K.M. Tohamy et al. [47] evaluated the influence of MgO replacing SiO_2 into SiO_2–Na_2O–CaO–P_2O_5–MgO glasses demonstrating that apatite layer formation decreased with increasing amount of MgO due to the formation of diopside. Similarly, in another study [48] CaP layers were found to be deposited on the lower MgO (8 to 2 mol%) content glass surface after 28 days of SBF study.

The FTIR spectra of the pastes, before immersion, i.e. zero-day, and after immersion, i.e. 14 days, in the SBF solution are shown in Figure 3b. The chemical groups associated with the formation of apatite are indicated in the spectra. The absorption bands at 460 and 1050 cm^{-1} are related to the Si-O-Si vibrations, while the chemical bond between glass Ca^{2+} and the carboxyl group from gelatin was detected at 1460 cm^{-1} in accordance with previous literature [15]. The hydrolysis observed by the bands at 1100 cm^{-1} and 940 cm^{-1} from the oxirane groups, as well as the band at 1254 cm^{-1} from the GPTMS epoxy groups [49] caused the formation of the Si-O-Si and Si-OH groups. These peaks overlap with the Si-O-Si from the bioactive glass and represent the formation of a bond between the epoxy groups of GPTMS and the amino groups from gelatin [50]. The bands marked in 560, 603, and 950 cm^{-1} indicated the presence of v4-$(PO_4)^{3-}$ thus giving confirmation of the apatite formation [50]. The absorption bands at 1630 and 3700-3000 cm^{-1} interval showed the presence of OH groups. Also, the 870, 1450 and 1510 cm^{1-} bands related to the CO_3^{2-} groups involved in the formation of type B carbonated apatite via replacing of phosphorus groups [10,50] were observed. In general, the intensities coming from the Mg-free paste peaks resulted as higher, thus suggesting that it is probably more bioactive due to the higher specific surface area of the Mg-free sample, and its lower bond strength. As a confirmation, the bond around 711 cm^{-1} related to calcite [51] was not found after 14 days for the BG-Gel-GPT20 specimens, thus confirming the results of the XRD characterization.

Finally, SEM-EDX images (Fig. 3c-d and Fig. 4) showed the morphology of the particles in the pastes, before and after the immersion in the SBF. Before immersion, the glass particles seem to be interconnected and bonded together by the polymers and the GPTMS. In general, regardless of the sample, the morphology of the particles is completely different before and after the immersion, showing a dense layer of spherical aggregates, ascribable to the *in vitro* formed hydroxyapatite. The EDX spectra shown in Figure 4 reported an increase in the intensity of Ca and P elements that can be an indication of the formation of a calcium phosphate-based phase on the surfaces of the pastes. Based on the XRD and FTIR results, the precipitated calcium phosphate can be claimed to be apatite. By replacing some Ca with Mg, apatite precipitates were

10

observed early on the surface of both composites after immersion in the SBF solution. Previous literature demonstrated that by substituting 5 mol.% of magnesium instead of calcium in 58S glass, the rates of apatite formation, cell proliferation, and cell differentiation were increased [52]. In another study, it was found that by adding 1 wt.% of MgO to the glass structure, a strong chemical bond with the bone was formed probably due to an increased bioactivity [53]. In conclusion, glasses' bioactivity can be influenced by the rate of dissolution and precipitation of the apatite layer, which is controlled by the composition and structure of the glass.

3.2 Biological characterization

3.2.1 Cytocompatibility

As debated, the here presented injectable pastes are aimed at small bone defects repair by direct injection into the injured site. So, the specimens' cytocompatibility was tested towards osteoblasts (MG-63) as cells representative for the bone tissue. To exclude any potential toxic effect due to the chemical composition or surface properties, cells were cultivated in direct contact with pastes. Polystyrene was used as control to compare test specimens' results as it represents the gold standard substrate for cells *in vitro* cultivation. Results are reported in Figure 5.

As can be seen, at both time-points the metabolic activity resulted as significantly higher (Fig. 5a, $p < 0.05$, indicated by *) for the cells cultivated in contact with pastes in comparison with polystyrene (poly) control, thus confirming the strong bioactive glasses' bioactivity even in the absence of biochemical stimulation such as ALP [54]. Moreover, by comparing the test groups, on day 7 the viability of the Mg-containing paste seeded cells was significantly higher than that of the Mg-free paste ($p < 0.05$, indicated by #). Based on the previous studies, Mg can favor cell adhesion, new bone formation, and metabolic activity of osteoblasts [15,47]. Also, literature showed that the proliferation and viability of osteoblasts as well as their ALP activity was superior if stimulated by Mg in comparison with cells cultivated with bulk medium [49]. Varanasi et al. [51] shown that the expression of collagen I, ALP, runx2, and osteocalcin increased by the dissolution of Mg-containing glass in cell culture [51]. Finally, SEM images (Fig. 5b) representative for 7 days direct cultivation showed that the cells are well attached and spread onto the surface displaying the typical stellate-like morphology of the osteoblasts.

3.2.2 Cells Migration

After evaluating pastes cytocompatibility towards osteoblasts cells cultivated directly onto top surface, a migration assay using fibroblasts was assessed. The aim of such evaluation is to simulate cells migration from the surrounding healthy tissue to the injured site filled by the paste: in this scenario, migrating cells must be able to move within the pores of the injected paste in order to fill it and promote the self-healing process while the composite acts as a temporary substrate. Accordingly, cells were seeded on the top of the

11

specimens and cultivated for 15 days; afterwards, specimens were vertically cut in two halves to analyze by SEM imaging the internal pores looking for cells migrated from the top layer (as schematized in Figure 6a). Results are reported in Figure 6.

As can be observed in the SEM images (Fig. 6b) fibroblasts were detected within the internal pores of the pastes, thus confirming that they were migrated from the top surface (where they were seeded) to the inner part of the cylindrical devices. The cytoskeleton elongation suggested that cells were able to adapt to the pastes' topography and chemistry, thus allowing for the pores filling representing a crucial step to support the self-healing process.

4. Conclusions

Obtained results suggested that the Ca ions substitution by the Mg ones can improve several properties of the bioactive glasses-based gelatin injectable pastes thanks to the higher ionic field strength of the former ion. So, despite a similar injectability, bioactive glasses doped with Mg showed better mechanical properties and higher bioactivity thanks to the possibility to control the release of Ca^{2+} thus reducing the formation of calcite in favor of the bone precursor apatite. Finally, pastes resulted as cytocompatible for osteoblasts as well as they were penetrated by migrating fibroblasts simulating the materials repopulation after implantation in the injured site. Therefore, the Mg-doped bioactive glasses appear as a promising tool for the treatment of small bone defects by direct injection.

References

[1] J.R. Jones, Reprint of: Review of bioactive glass: From Hench to hybrids, Acta Biomater. 23 (2015) S53-82. https://doi.org/10.1016/j.actbio.2015.07.019.

[2] M. Cazzola, E. Verné, A. Cochis, R. Sorrentino, B. Azzimonti, E. Prenesti, L. Rimondini, S, Ferraris. Bioactive glasses functionalized with polyphenols: in vitro interactions with healthy and cancerous osteoblast cells, J. Mater. Sci. 52 (2017) 9211-9223. https://doi.org/10.1007/s10853-017-0872-5.

[3] M. Miola, F. Laviano, R. Gerbaldo, M. Bruno, A. Lombardi, A. Cochis, L. Rimondini, E. Verné. Composite bone cements for hyperthermia: modeling and characterization of magnetic, calorimetric and in vitro heating properties, Ceram. Int. 43 (2017) 4831-4840. https://doi.org/10.1016/j.ceramint.2016.12.049.

[4] L.L. Hench, Bioceramics: From Concept to Clinic. Am. Ceram. Soc. 74 (1991) 1487–1510. https://doi.org/10.1111/j.1151-2916.1991.tb07132.x.

[5] B. Jeong, S.W. Kim, Y.H. Bae, Thermosensitive sol–gel reversible hydrogels, Adv. Drug Deliv. Rev. 54 (2002) 37–51. https://doi.org/10.1016/s0169-409x(01)00242-3.

[6] M. Sohrabi, S. Hesaraki, A. Kazemzadeh, Injectable Bioactive Glass/Polysaccharide Polymers Nanocomposites for Bone Substitution, Key Eng. Mater. 614 (2014) 41–46. https://doi.org/10.4028/www.scientific.net/kem.614.41.

[7] D. Vukajlovic, J. Parker, O. Bretcanu, K. Novakovic, Chitosan based polymer/bioglass composites for tissue engineering applications, Mater. Sci. Eng. C. 96 (2019) 955–967. https://doi.org/10.1016/j.msec.2018.12.026.

[8] T. Irimia, C.-E. Dinu-Pîrvu, M. Ghica, D. Lupuleasa, D.-L. Muntean, D. Udeanu, L. Popa, Chitosan-Based In Situ Gels for Ocular Delivery of Therapeutics: A State-of-the-Art Review, Mar. Drugs. 16 (2018) 373. https://doi.org/10.3390/md16100373.

[9] M.N. Sundaram, S. Amirthalingam, U. Mony, P.K. Varma, R. Jayakumar, Injectable chitosan-nano bioglass composite hemostatic hydrogel for effective bleeding control, Int. J. Biol. Macromol. 129 (2019) 936–943. https://doi.org/10.1016/j.ijbiomac.2019.01.220.

[10] M. Sohrabi, S. Hesaraki, A. Kazemzadeh, M. Alizadeh, Development of injectable biocomposites from hyaluronic acid and bioactive glass nano-particles obtained from different sol–gel routes, Mater. Sci. Eng. C. 33 (2013) 3730–3744. https://doi.org/10.1016/j.msec.2013.05.005.

[11] M. Sohrabi, S. Hesaraki, A. Kazemzadeh, The influence of polymeric component of bioactive glass-based nanocomposite paste on its rheological behaviors and in vitro responses: Hyaluronic acid versus sodium alginate, J. Biomed. Mater. Res. B Appl. Biomater. 102(3) (2014) 561-573.

[12] H. Luo, Y. Zhang, Z. Wang, Z. Yang, J. Tu, Z. Liu, F. Yao, G. Xiong, Y. Wan, Constructing three-dimensional nanofibrous bioglass/gelatin nanocomposite scaffold for enhanced mechanical and biological performance, Chem. Eng. J. 326 (2017) 210–221. https://doi.org/10.1016/j.cej.2017.05.115.

[13] S.C.G. Leeuwenburgh, J. Jo, H. Wang, M. Yamamoto, J.A. Jansen, Y. Tabata, Mineralization, Biodegradation, and Drug Release Behavior of Gelatin/Apatite Composite Microspheres for Bone Regeneration, Biomacromolecules. 11 (2010) 2653–2659. https://doi.org/10.1021/bm1006344.

[14] M. Peter, N.S. Binulal, S.V. Nair, N. Selvamurugan, H. Tamura, R. Jayakumar, Novel biodegradable chitosan–gelatin/nano-bioactive glass ceramic composite scaffolds for alveolar bone tissue engineering, Chem. Eng. J. 158 (2010) 353–361. https://doi.org/10.1016/j.cej.2010.02.003.

[15] M. Sohrabi, B. Eftekhari Yekta, H.R. Rezaie, M.R. Naimi-Jamal, Rheology, injectability, and bioactivity of bioactive glass containing chitosan/gelatin, nano pastes, J. Appl. Polym. Sci. 137 (2020) 49240. https://doi.org/10.1002/app.49240.

[16] C.D.F. Moreira, S.M. Carvalho, H.S. Mansur, M.M. Pereira, Thermogelling chitosan–collagen–bioactive glass nanoparticle hybrids as potential injectable systems for tissue engineering, Mater. Sci. Eng. C. 58 (2016) 1207–1216. https://doi.org/10.1016/j.msec.2015.09.075.

[17] D.U. Tulyaganov, A.A. Reddy, R. Siegel, E. Ionescu, R. Riedel, J.M.F. Ferreira, Synthesis and in vitro bioactivity assessment of injectable bioglass–organic pastes for bone tissue repair, Ceram. Int. 41 (2015) 9373–9382. https://doi.org/10.1016/j.ceramint.2015.03.312.

[18] A.K. Miri, N. Muja, N.O. Kamranpour, W.C. Lepry, A.R. Boccaccini, S.A. Clarke, S.N. Nazhat, Ectopic bone formation in rapidly fabricated acellular injectable dense collagen-Bioglass hybrid scaffolds via gel aspiration-ejection, Biomaterials. 85 (2016) 128–141. https://doi.org/10.1016/j.biomaterials.2016.01.047.

[19] H. Jiankang, L. Dichen, L. Yaxiong, Y. Bo, L. Bingheng, L. Qin, Fabrication and characterization of chitosan/gelatin porous scaffolds with predefined internal microstructures, Polymer. 48 (2007) 4578–4588. https://doi.org/10.1016/j.polymer.2007.05.048.

[20] T. Wang, L. Chen, T. Shen, D. Wu, Preparation and properties of a novel thermo-sensitive hydrogel based on chitosan/hydroxypropyl methylcellulose/glycerol, Int. J. Biol. Macromol. 93 (2016) 775–782. https://doi.org/10.1016/j.ijbiomac.2016.09.038.

[21] M. Farokhi, N. Nezafati, M. Heydari, S. Hesaraki, Use of epoxypropoxy-propyl-trimethoxysilane in the fabrication of bioactive gelatin microspheres using an emulsification method, J. Membr. Sci. 51 (2016) 9356–9366. https://doi.org/10.1007/s10853-016-0182-3.

[22] A.-C. Chao, Preparation of porous chitosan/GPTMS hybrid membrane and its application in affinity sorption for tyrosinase purification with Agaricus bisporus, J. Membr. Sci. 311 (2008) 306–318. https://doi.org/10.1016/j.memsci.2007.12.032.

[23] A.J. Salinas, J. Román, M. Vallet-Regi, J.M. Oliveira, R.N. Correia, M.H. Fernandes, In vitro bioactivity of glass and glass-ceramics of the 3CaO·P2O5–CaO·SiO2–CaO·MgO·2SiO2 system, Biomaterials. 21 (2000) 251–257. https://doi.org/10.1016/s0142-9612(99)00150-7.

[24] J. Roman, A.J. Salinas, M. Vallet-Regi, J.M. Oliveira, R.N. Correia, M.H. Fernandes, Role of acid attack in the in vitro bioactivity of a glass-ceramic of the 3CaO·P2O5-CaO·SiO2-CaO·MgO·2SiO2 system, Biomaterials. 22 (2001) 2013–2019. https://doi.org/10.1016/s0142-9612(00)00387-2.

[25] M.M. Pereira, A.E. Clark, L.L. Hench, Effect of Texture on the Rate of Hydroxyapatite Formation on Gel-Silica Surface, J. Am. Ceram. Soc. 78 (1995) 2463–2468. https://doi.org/10.1111/j.1151-2916.1995.tb08686.x.

[26] M. Bellantone, H.D. Williams, L.L. Hench, Broad-Spectrum Bactericidal Activity of Ag2O-Doped Bioactive Glass, Antimicrob. Agents Chemother. 46 (2002) 1940–1945. https://doi.org/10.1128/aac.46.6.1940-1945.2002.

[27] S.J. Watts, R.G. Hill, M.D. O'Donnell, R.V. Law, Influence of magnesia on the structure and properties of bioactive glasses, J. Non-Cryst. Solids. 356 (2010) 517–524. https://doi.org/10.1016/j.jnoncrysol.2009.04.074.

[28] E. Gentleman, M.M. Stevens, R.G. Hill, D.S. Brauer, Surface properties and ion release from fluoride-containing bioactive glasses promote osteoblast differentiation and mineralization in vitro, Acta Biomater. 9 (2013) 5771–5779. https://doi.org/10.1016/j.actbio.2012.10.043.

[29] A. Balamurugan, G. Balossier, S. Kannan, J. Michel, A.H.S. Rebelo, J.M.F. Ferreira, Development and in vitro characterization of sol–gel derived CaO–P2O5–SiO2–ZnO bioglass, Acta Biomater. 3 (2007) 255–262. https://doi.org/10.1016/j.actbio.2006.09.005.

[30] U. Gross, V. Strunz, The interface of various glasses and glass ceramics with a bony implantation bed, J. Biomed. Mater. Res. 19 (1985) 251–271. https://doi.org/10.1002/jbm.820190308.

[31] D.S. Brauer, N. Karpukhina, M.D. O'Donnell, R.V. Law, R.G. Hill, Fluoride-containing bioactive glasses: Effect of glass design and structure on degradation, pH and apatite formation in simulated body fluid, Acta Biomater. 6 (2010) 3275–3282. https://doi.org/10.1016/j.actbio.2010.01.043.

[32] V. Cannillo, A. Sola, Potassium-based composition for a bioactive glass, Ceram. Int. 35 (2009) 3389–3393. https://doi.org/10.1016/j.ceramint.2009.06.011.

[33] Y. Zhu, Y. Zhang, C. Wu, Y. Fang, J. Yang, S. Wang, The effect of zirconium incorporation on the physiochemical and biological properties of mesoporous bioactive glasses scaffolds, Microporous Mesoporous Mater. 143 (2011) 311–319. https://doi.org/10.1016/j.micromeso.2011.03.007.

[34] M.T. Souza, M.C. Crovace, C. Schröder, H. Eckert, O. Peitl, E.D. Zanotto, Effect of magnesium ion incorporation on the thermal stability, dissolution behavior and bioactivity in Bioglass-derived glasses, J. Non-Cryst. Solids. 382 (2013) 57–65. https://doi.org/10.1016/j.jnoncrysol.2013.10.001.

[35] A. Hoppe, N.S. Güldal, A.R. Boccaccini, A review of the biological response to ionic dissolution products from bioactive glasses and glass-ceramics, Biomaterials. 32 (2011) 2757–2774. https://doi.org/10.1016/j.biomaterials.2011.01.004.

[36] J.M. Oliveira, R.N. Correia, M.H. Fernandes, J. Rocha, Influence of the CaO/MgO ratio on the structure of phase-separated glasses: a solid state 29Si and 31P MAS NMR study, J. Non-Cryst. Solids. 265 (2000) 221–229. https://doi.org/10.1016/s0022-3093(99)00957-6.

[37] J. Ma, C.Z. Chen, D.G. Wang, J.H. Hu, Effect of magnesia on structure, degradability and in vitro bioactivity of CaO–MgO–P2O5–SiO2 system ceramics, Mater. Lett. 65 (2011) 130–133. https://doi.org/10.1016/j.matlet.2010.09.040.

[38] Y. Ebisawa, T. Kokubo, K. Ohura, T. Yamamuro, Bioactivity of CaO SiO2-based glasses:in vitro evaluation, Journal of Materials Science: J Mater Sci Mater Med. 1 (1990) 239–244. https://doi.org/10.1007/bf00701083.

[39] T. Kasuga, K. Nakagawa, M. Yoshida, E. Miyade, Compositional dependence of formation of an apatite layer on glass-ceramics in simulated physiological solution, J. Mater. Sci. 22 (1987) 3721–3724. https://doi.org/10.1007/bf01161484.

15

[40] J. Massera, L. Hupa, M. Hupa, Influence of the partial substitution of CaO with MgO on the thermal properties and in vitro reactivity of the bioactive glass S53P4, J. Non-Cryst. Solids. 358 (2012) 2701–2707. https://doi.org/10.1016/j.jnoncrysol.2012.06.032.

[41] D. Pereira, S. Cachinho, M.C. Ferro, M.H.V. Fernandes, Surface behaviour of high MgO-containing glasses of the Si–Ca–P–Mg system in a synthetic physiological fluid, J. Eur. Ceram. Soc. 24 (2004) 3693–3701. https://doi.org/10.1016/j.jeurceramsoc.2004.02.006.

[42] J.M. Oliveira, R.N. Correia, M.H. Fernandes, Effects of Si speciation on the in vitro bioactivity of glasses, Biomaterials. 23 (2002) 371–379. https://doi.org/10.1016/s0142-9612(01)00115-6.

[43] M. Vallet-Regí, A.J. Salinas, J. Román, M. Gil, Effect of magnesium content on the in vitro bioactivity of CaO-MgO-SiO2-P2O5 sol-gel glasses, J. Mater. Chem. 9 (1999) 515–518. https://doi.org/10.1039/a808679f.

[44] T. Kokubo, H. Takadama, How useful is SBF in predicting in vivo bone bioactivity?, Biomaterials. 27 (2006) 2907–2915. https://doi.org/10.1016/j.biomaterials.2006.01.017.

[45] X.H. Zhang, Y.L. Yue, H.T. Wu, Effects of cation field strength on structure and properties of boroaluminosilicate glasses, Mater. Res. Innov. 17 (2013) 212–217. https://doi.org/10.1179/1433075x12y.0000000051.

[46] R.K.H. Seah, M. Garland, J.S.C. Loo, E. Widjaja, Use of Raman Microscopy and Multivariate Data Analysis to Observe the Biomimetic Growth of Carbonated Hydroxyapatite on Bioactive Glass, Anal. Chem. 81 (2009) 1442–1449. https://doi.org/10.1021/ac802234t.

[47] K. Tohamy, M. El-Okr, A. Ali, I.E. Soliman, M. El-Gohary, Effect of Mg2+ Doping on Formation of Apatite Layer by Bioactive Sol-Gel Glass-Ceramic, Egyptian Journal of Biomedical Engineering and Biophysics. 12 (2011) 69–85. https://doi.org/10.21608/ejbbe.2011.1188.

[48] M.T. Islam, K.M.Z. Hossain, N. Sharmin, A.J. Parsons, I. Ahmed, Effect of magnesium content on bioactivity of near invert phosphate-based glasses, Int. J. Appl. Glass Sci. 8 (2017) 391–402. https://doi.org/10.1111/ijag.12320.

[49] S. Ma, W. Liu, Z. Wei, H. LI, Mechanical and Thermal Properties and Morphology of Epoxy Resins Modified by a Silicon Compound, J. Macromol. Sci. A. 47 (2010) 1084–1090. https://doi.org/10.1080/10601325.2010.511522.

[50] S. Hesaraki, F. Moztarzadeh, N. Nezafati, Evaluation of a bioceramic-based nanocomposite material for controlled delivery of a non-steroidal anti-inflammatory drug, Med Eng Phys. 31 (2009) 1205–1213. https://doi.org/10.1016/j.medengphy.2009.07.019.

[51] M. Mami, A. Lucas-Girot, H. Oudadesse, R. Dorbez-Sridi, F. Mezahi, E. Dietrich, Investigation of the surface reactivity of a sol–gel derived glass in the ternary system SiO2–CaO–P2O5, Appl. Surf. Sci. 254 (2008) 7386–7393. https://doi.org/10.1016/j.apsusc.2008.05.340.

16

[52] A. Moghanian, A. Sedghi, A. Ghorbanoghli, E. Salari, The effect of magnesium content on in vitro bioactivity, biological behavior and antibacterial activity of sol–gel derived 58S bioactive glass, Ceram. Int. 44 (2018) 9422–9432. https://doi.org/10.1016/j.ceramint.2018.02.159.

[53] E. Jallot, Role of magnesium during spontaneous formation of a calcium phosphate layer at the periphery of a bioactive glass coating doped with MgO, Appl. Surf. Sci. 211 (2003) 89–95. https://doi.org/10.1016/s0169-4332(03)00179-x.

[54] E. Vernè, S. Ferraris, C. Vitale-Brovarone, A. Cochis, L. Rimondini. Bioactive glass functionalized with alkaline phosphatase stimulates bone extracellular matrix deposition and calcification in vitro, Appl. Surf. Sci. 313 (2014) 372-381. https://doi.org/10.1016/j.apsusc.2014.06.001

Figure Legends

Figure 1. The disintegration resistance (Dr) test in SBF immersion demonstrated a higher resistance to degradation from the Mg-doped composites (BG-Mg-Gel-GPT20) in comparison to the bulk ones (BG-Gel-GPT20) (a). This is due to the superior structural stability conferred by the Mg ions linking the polymer chains (b) that ameliorated the bond between the bioactive glass (BG) and the gelatin (Gel) as schematized in (c).

Figure 2. Rheology. The use of GPTMS as cross linker allowed for bond with gelatin chains by the silanol groups (a). The presence of Mg (BG-Mg-Gel-GPT20) improved the storage and loss modules (b) as well as the complex viscosity (c) in comparison with the bulk BG-Gel-GPT20.

Figure 3. Bioactivity. The XRD patterns (a) showed the presence of apatite after immersion in SBF for both pastes as confirmed by the FTIR spectra too (b). SEM images of BG-Gel-GPT20 (c) and BG-Mg-Gel-GPT20 (d) provided a visual proof of the apatite crystals formation.

Figure 4. EDX spectra of control (a-b, BG-Gel-GPT20) and Mg-doped specimens (c-d, BG-Mg-Gel-GPT20) before and after immersion in SBF.

Figure 5. Cytocompatibility. Pastes demonstrated to be bioactive by significantly improving osteoblasts metabolism in comparison with polystyrene (poly) control (a, $p<0.05$ indicated by *); moreover, Mg (BG-Mg-Gel-GPT20) led to a higher metabolic activity after 7 days in comparison to the BG-Gel-GPT20 bulk material ($p<0.05$, indicated by #). SEM images confirmed cells' adhesion and spread displaying the typical osteoblast stellate morphology.

Figure 6. Migration assay. By analyzing pastes internal pores using SEM imaging (schematized in a by red circles) it was possible to observe cells migrating from the top to the internal part of the devices adhering and spreading across pores (b) after 15 days cultivation.

17

Composite	BG (g)	Gel (g)	GPTMS (wt.%)
BG-Mg-Gel-GPT20	0.25	1	20
BG-Gel-GPT20	0.25	1	20

Table 1. Bioactive glass (BG) - gelatin (Gel) - trimethoxysilane 3-glycidyloxypropyl) (GPTMS) composites.
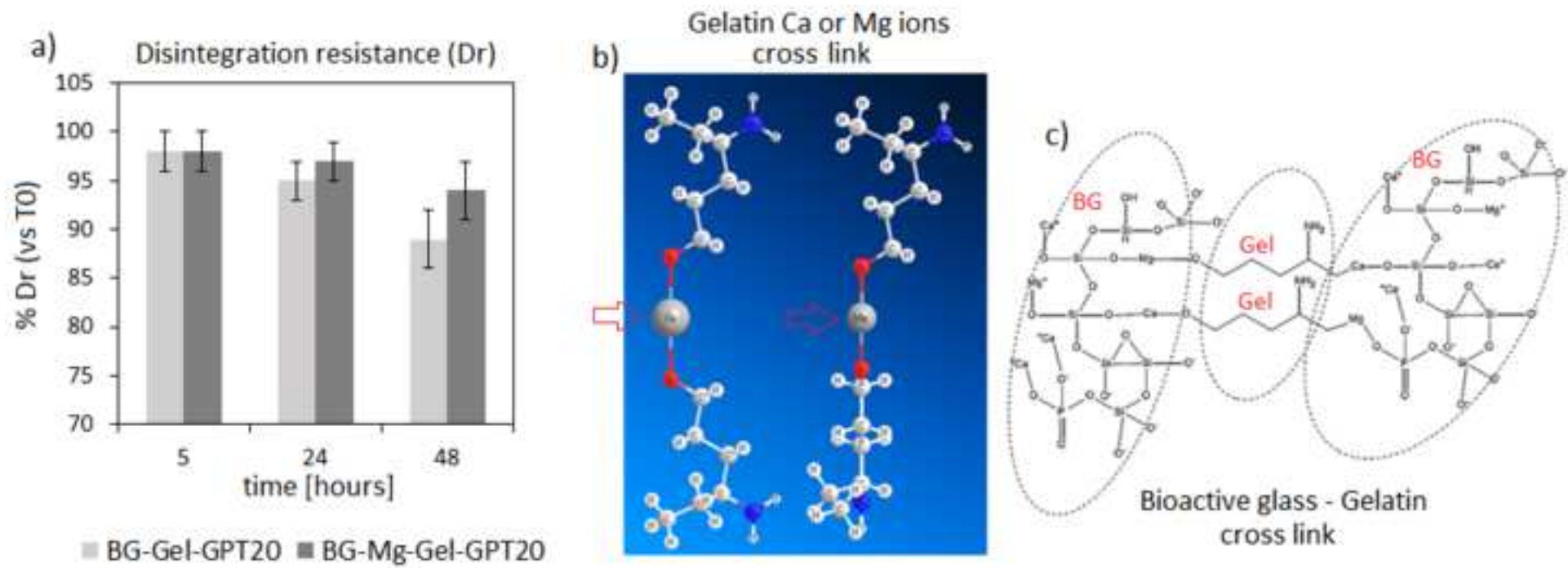
1
2
3
4
5
6
7
8
9
10
11
12
13
14
15
16
17
18
19
20
21
22
23
24
25
26
27
28
29
30
31
32
33
34
35
36
37
38
39
40
41
42
43
44
45
46
47
48
49
50
51
52
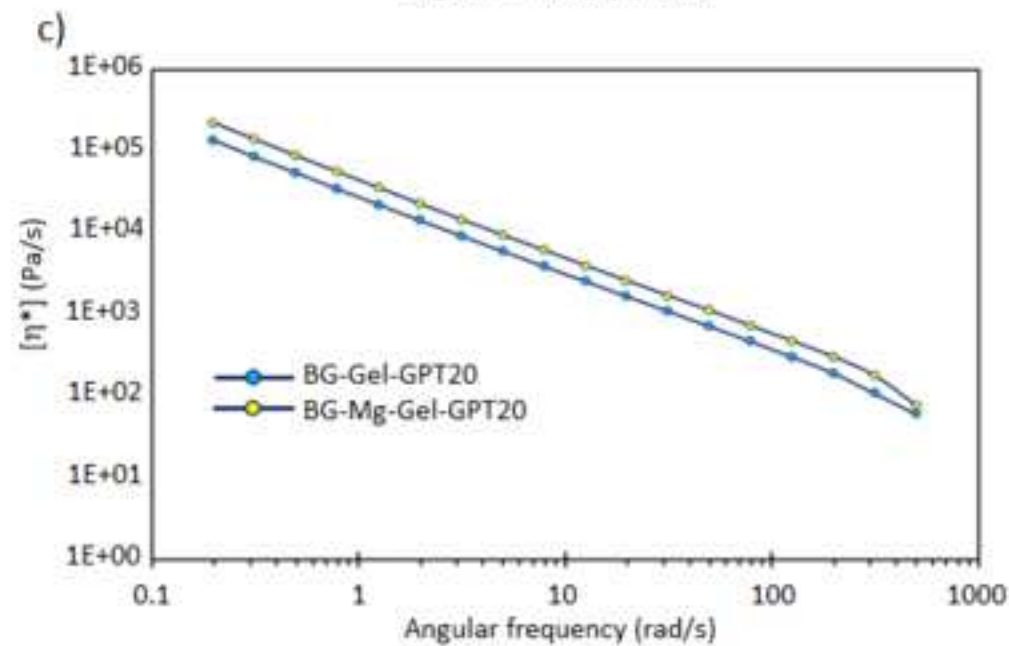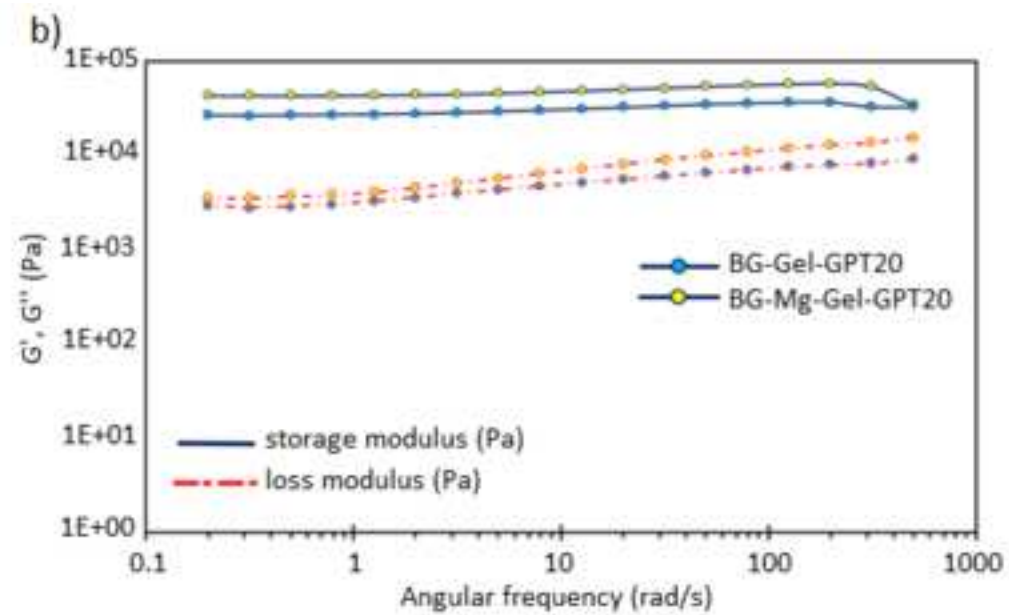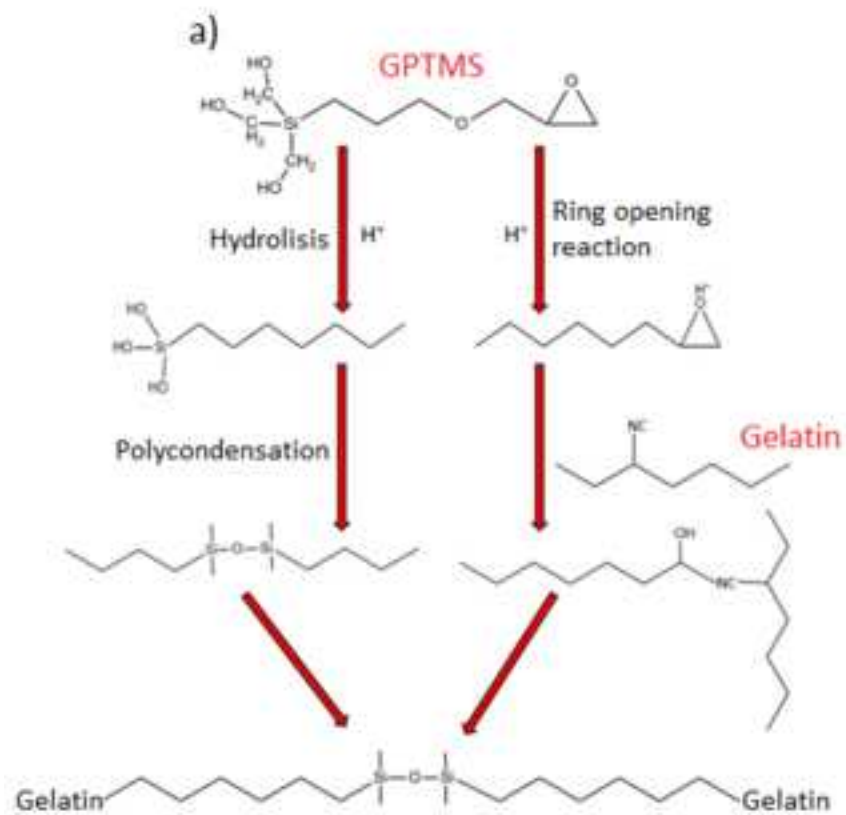53
54
55
56
57
58
59
60
61
62
63
64
65

Composite	BET		XRD	SEM	
BG-Gel-GPT20	pore volume specific surface area size of average pores	0.602 (cm^3/g) 123.139(m^2/g) 18.217 (nm)	amorphous	particle size	50 (nm)
BG-Mg-Gel-GPT20	pore volume specific surface area size of average pores	0.634 (cm^3/g) 109.104(m^2/g) 23.036 (nm)	amorphous	particle size	100 (nm)

Table 2. Composites physical-chemical characterization summary.

Composite	Injection force (N)	Injectability (%)
BG-Gel-GPT20	5±2	97±1
BG-Mg-Gel-GPT20	5±3	98±2

Table 3. Applied force and injection percentage (2 mm diameter needle). Results are expressed as means ± standard deviations of 3 replicates.

Composite	$G'_{(Pa)}$	$G''_{(Pa)}$	$\eta^*_{(max)\,(Pa/s)}$
BG-Gel-GPT20	268×10^2	2920	136×10^3
BG-Mg-Gel-GPT20	434×10^2	3610	219×10^3

Table 4. Storage module (G'), loss module (G''), and viscosity (η*) of composites.

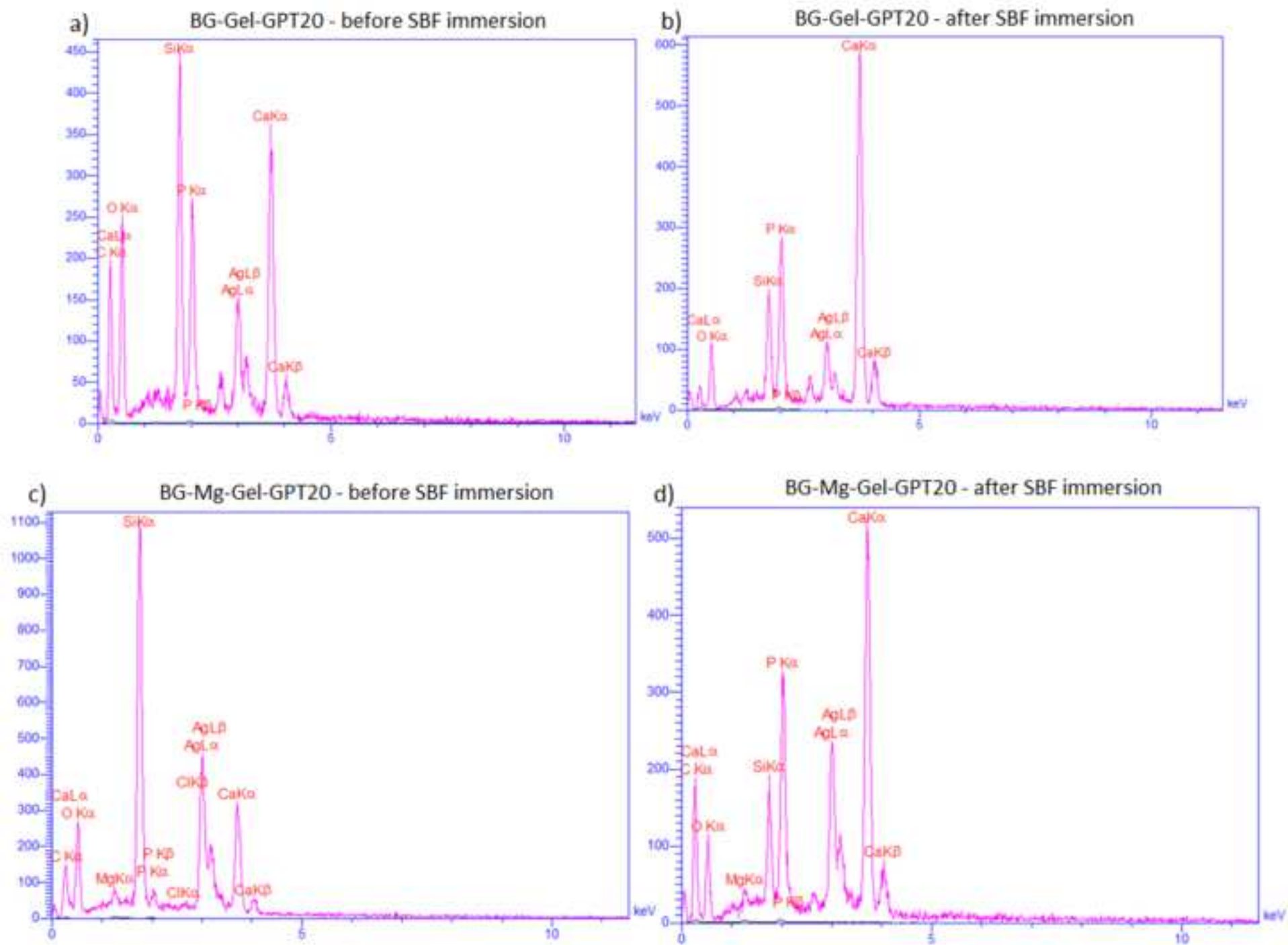Figure 1   Click here to access/download;Figure;Figure 1.tif

a) Disintegration resistance (Dr)

BG-Gel-GPT20   BG-Mg-Gel-GPT20

b) Gelatin Ca or Mg ions cross link

c) Bioactive glass - Gelatin cross link

Figure 2

Click here to access/download;Figure;Figure 2.tif

Figure 3

Click here to access/download;Figure;Figure 3.tif ⬇

Figure 4   Click here to access/download;Figure;Figure 4.tif ±

a) BG-Gel-GPT20 - before SBF immersion
b) BG-Gel-GPT20 - after SBF immersion
c) BG-Mg-Gel-GPT20 - before SBF immersion
d) BG-Mg-Gel-GPT20 - after SBF immersion

Figure 5

Click here to access/download;Figure;Figure 5.tif ⬇

a) Cells Viability

b) BG-Gel-GPT20   BG-Mg-Gel-GPT20

day 7

Figure 6

Click here to access/download;Figure;Figure 6.tif

UPO
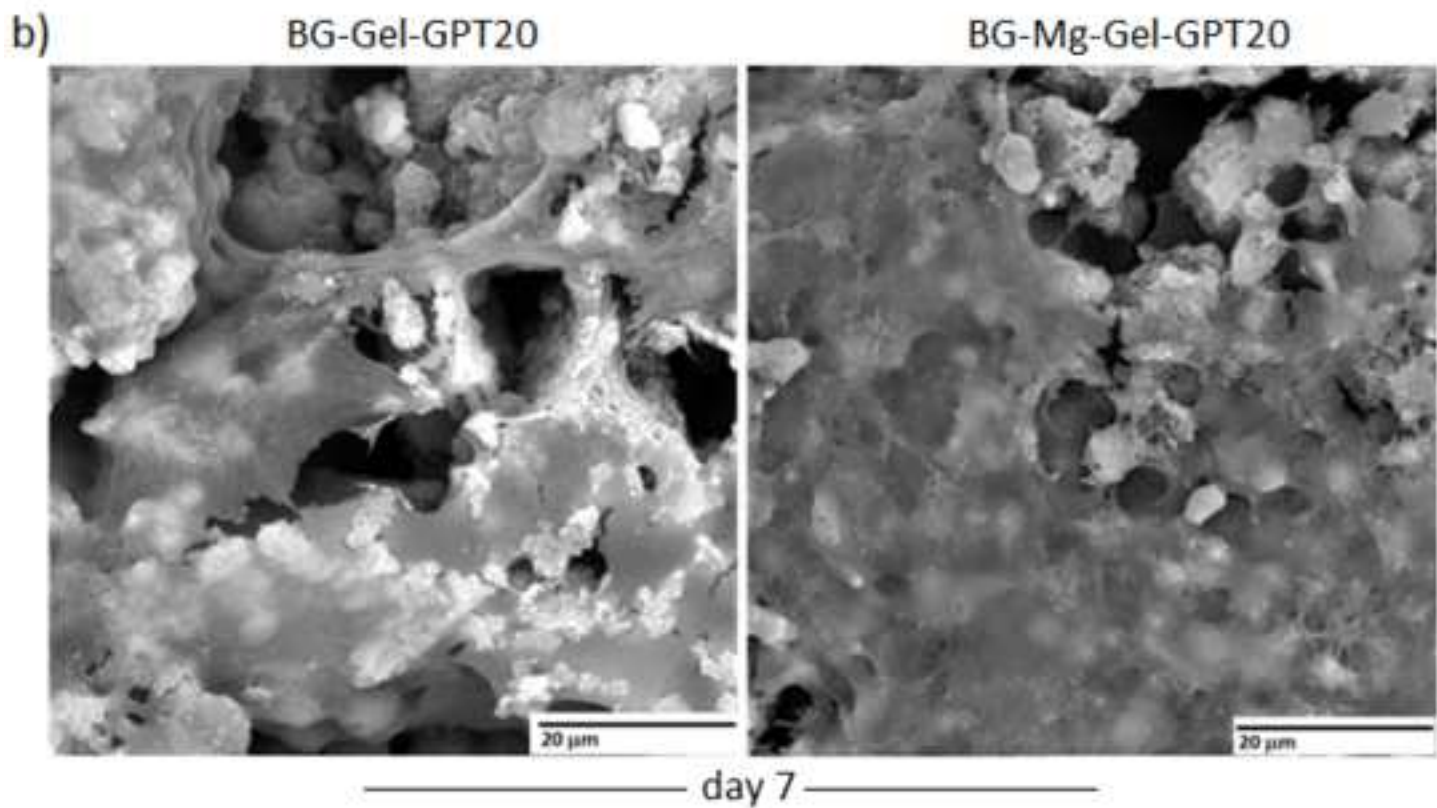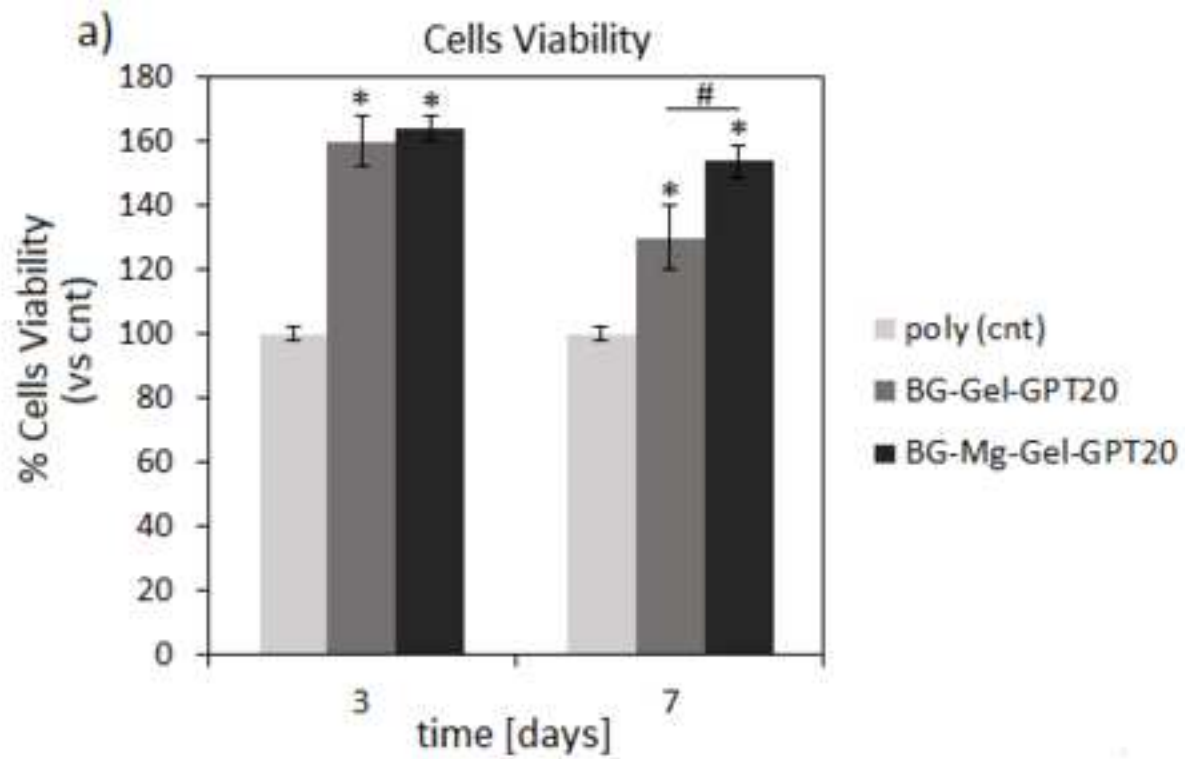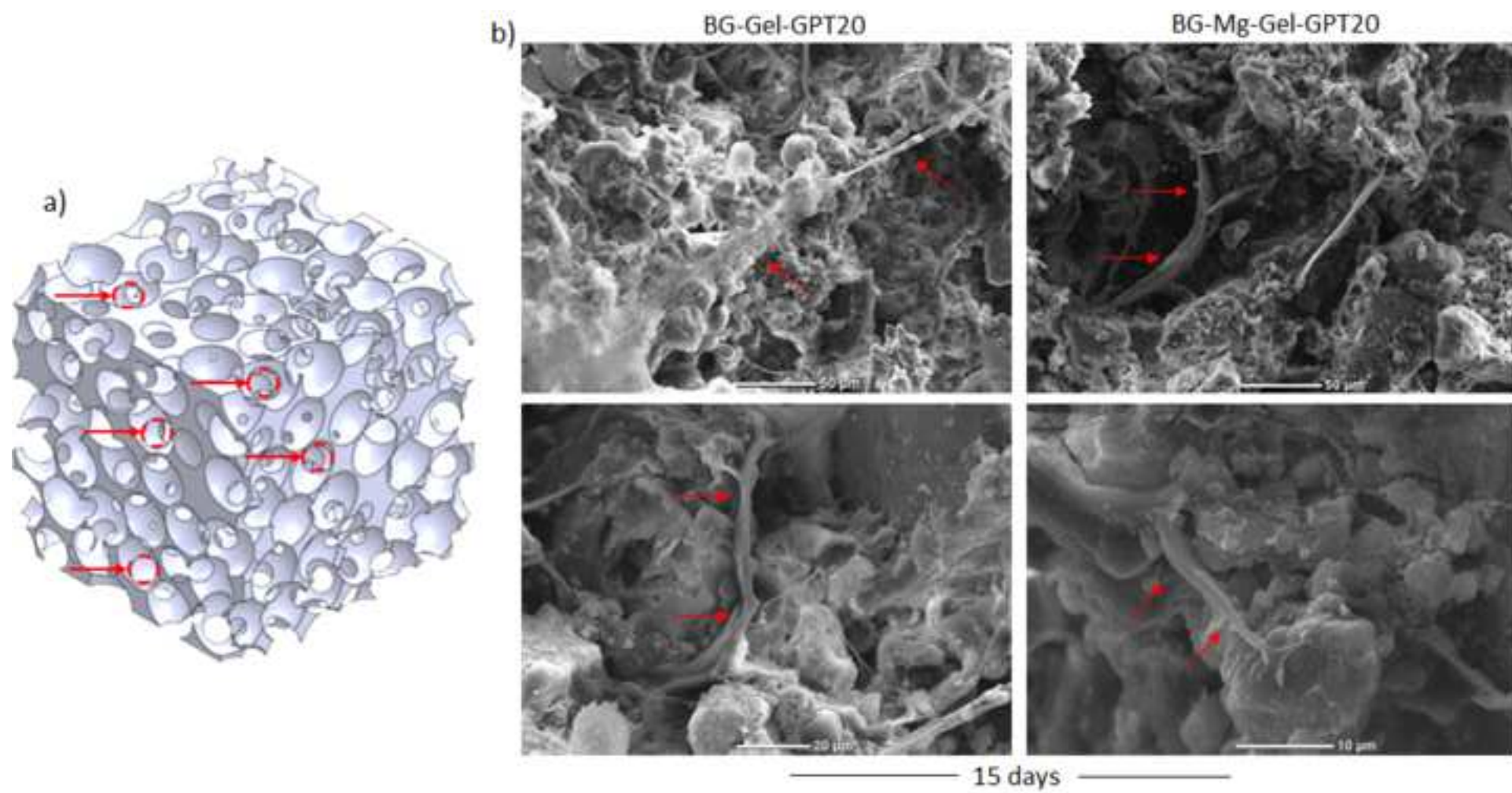UNIVERSITÀ DEL PIEMONTE ORIENTALE

Iran University of
Science &Technology

Conflict of Interest Declaration:

Regarding the submission of the original article entitled "*The effect of Magnesium on bioactivity, rheology and biology behaviors of injectable bioactive glass-gelatin-3-glycidyloxypropyl trimethoxysilane nanocomposite-paste for small bone defects repair*" by Mehri Sohrabi, Bijan Eftekhari Yekta, Hamidreza Rezaie, Mohammad Reza Naimi-Jamal, Ajay Kumar, Andrea Cochis, Marta Miola and Lia Rimondini,

We confirm that the manuscript is original, that it has been approved by all the Authors and that it is not actually under the evaluation of any other Journal.

We confirm that the Authors have no conflicts of interest.

Sincerely,
the corresponding Authors,

Prof. Bijan Eftekhari Yekta

Prof. Lia Rimondini